Dihydroxylation of four- and five-ring aromatic hydrocarbons by the naphthalene dioxygenase from Sphingomonas CHY-1

Yves Jouanneau, Christine Meyer, Nicolas Duraffourg

HAL Id: hal-01260091

https://hal.archives-ouvertes.fr/hal-01260091

Submitted on 21 Jan 2016

1 **Dihydroxylation of four- and five-ring aromatic hydrocarbons by the naphthalene**

2 **dioxygenase from *Sphingomonas* CHY-1**

3

4

5

6 Yves Jouanneau[1,2,3], Christine Meyer[1,2,3], and Nicolas Duraffourg[1,2,3]

7

8 [1] CEA, DSV, iRTSV, Laboratoire de Chimie et Biologie des Métaux, F-38054 Grenoble,

9 France.

10 [2] CNRS, UMR 5249, Grenoble, France.

11 [3] Univ. Grenoble Alpes, F-38000 Grenoble, France

12

13

14 Running title : Dioxygenation of 4- and 5-ring PAHs

15

16

17 Corresponding author:

18 Yves Jouanneau

19 LCBM/iRTSV, CEA-Grenoble

20 F-38054 Grenoble Cedex 9, France.

21 Tel. : 33 (0)4 38 78 43 10; Fax : 33 (0)4 38 78 54 87

22 Email : yves.jouanneau@cea.fr

23

1   **ABSTRACT**

2   The naphthalene dioxygenase from *Sphingomonas* CHY-1 exhibits extremely broad substrate

3   specificity toward polycyclic aromatic hydrocarbons (PAHs). In a previous study, the

4   catalytic rates of oxidation of 9 PAHs were determined using the purified dioxygenase, but

5   the oxidation products formed from 4- to 5-ring hydrocarbons were incompletely

6   characterized. Here, we reexamined PAH oxygenation reactions using *Escherichia coli*

7   recombinant cells overproducing strain CHY-1 dioxygenase. Hydroxylated products

8   generated by the dioxygenase were purified, and characterized by means of GC-MS, UV

9   absorbance as well as ^{1}H and ^{13}C-NMR spectroscopy. Fluoranthene was converted to 3

10   dihydrodiols, the most abundant of which was identified as *cis*-7,8-dihydroxy-7,8-

11   dihydrofluoranthene. This diol turned out to be highly unstable, converting to 8-

12   hydroxyfluoranthene by spontaneous dehydration. The dioxygenase also catalyzed

13   dihydroxylations on the C2-C3, and presumably the C1-C2 positions, although at much lower

14   rates.   Benz[a]anthracene was converted into three dihydrodiols, hydroxylated in positions

15   C1-C2, C8-C9 and C10-C11, and one *bis-cis*-dihydrodiol. The latter compound was identified

16   as *cis,cis*-1,2,10,11-tetrahydroxy-1,2,10,11-tetrahydrobenz[a]anthracene, which resulted from

17   the subsequent dioxygenation of the 1,2- or 10,11-dihydrodiols. Chrysene dioxygenation

18   yielded a single diol identified as *cis*-3,4-dihydroxy-3,4-dihydrochrysene, which underwent

19   further oxidation to give *cis,cis*-3,4,9,10 chrysene tetraol. Pyrene was a poor substrate for the

20   CHY-1 dioxygenase and gave a single dihydrodiol hydroxylated on C4 and C5, whereas

21   benzo[a}pyrene was converted to two dihydrodiols, one of which was identified as *cis*-9,10-

22   dihydrodiol. The selectivity of the dioxygenase is discussed in the light of the known 3D

23   structure of its catalytic component, and compared to that of the few enzymes able to attack 4-

24   and 5-ring PAHs.

25   Key words : Ring hydroxylation ; dioxygenase ; *cis*-dihydrodiols ; PAH ; regioselectivity

INTRODUCTION

Polycyclic aromatic hydrocarbons (PAHs) are a class of hazardous hydrophobic compounds that are widespread in the environment. Due to their high chemical stability and low aqueous solubility, they persist for long times on contaminated sites, especially high molecular weight (HMW) PAHs that are composed of 4 to 6 rings. Microbial biodegradation is mainly responsible for natural attenuation and is exploited in several strategies of bioremediation (Bamforth and Singleton 2005; Lu et al. 2011). PAH biodegradation pathways have been extensively studied with specialized microorganisms, most often isolated from contaminated sites. In bacteria, the catabolic pathways leading to the complete mineralization of 2- and 3-ring PAHs has been described in detail (Doyle et al. 2008; Peng et al. 2008). In contrast, the degradation of HMW-PAHs is much less understood, except in a *Mycobacterium* strain where the metabolism of pyrene and fluoranthene has been thoroughly investigated (Kim et al. 2007; Kweon et al. 2007). The lower level of understanding of HMW-PAHs degradation, might be due to two main reasons: (i) only a few bacterial isolates were found capable of degrading such compounds, including Sphingomonads (Kunihiro et al. 2013; Lyu et al. 2014; Maeda et al. 2014; Story et al. 2001; Willison 2004) and *Mycobacteria* (Heitkamp et al. 1988; Krivobok et al. 2003; Schneider et al. 1996; Vila et al. 2001), and (ii) the degradation pathways are complex and often involve multiple routes (Kweon et al. 2007; Rehmann et al. 2001). In addition, some PAHs like benzo[a]pyrene are thought to be degraded through co-metabolism (Juhasz and Naidu 2000).

The initial step in the oxidative degradation of PAHs by bacteria is catalyzed by specific metalloenzymes called ring-hydroxylating dioxygenases (RHDs). They are multi-component enzymes, most often comprising three elements, a NAD(P)H-oxidoreductase, a ferredoxin and an oxygenase that carries the active site (Jouanneau et al. 2011; Parales and Resnick 2006). The oxygenase component is generally an hexamer $\alpha_3\beta_3$, where each alpha subunit

1 binds a Rieske-type [2Fe-2S] cluster and a mononuclear ferrous iron center, which is the

2 catalytic site of the enzyme. The RHD enzymatic reaction involves several steps, including

3 binding of the substrate, electron transfer from NAD(P)H to the active site, dioxygen

4 activation, and hydroxylation of two adjacent carbon atoms of the substrate to give a *cis*-

5 dihydrodiol (Karlsson et al. 2003).

6 RHDs form a large enzyme family that has been divided into four or five subgroups,

7 essentially based on comparisons of their alpha subunit sequences (Kweon et al. 2008; Nam et

8 al. 2001). Two subgroups appeared to be composed of PAH-specific RHDs, which differ

9 depending on whether they belonged to Gram-positive or Gram-negative bacteria (Jouanneau

10 et al. 2011; Kweon et al. 2008). Among the few RHDs able to attack HMW-PAHs, the

11 naphthalene dioxygenase from *Sphingomonas* CHY-1 is one of the best-characterized enzyme.

12 Its structural genes have been cloned and overexpressed in *Escherichia coli,* thus producing a

13 functional enzyme able to oxidize 2- to 4-ring PAHs (Demaneche et al. 2004). The RHD was

14 later purified and its catalytic activity towards 9 PAHs ranging from 2 to 5 rings was

15 characterized with respect to reaction rates and the nature of the dihydrodiols formed

16 (Jouanneau et al. 2006). These studies showed that some 3- or 4-ring substrates like fluorene

17 and benz[a]anthracene were converted to multiple hydroxylated products. It was also

18 observed that the dioxygenase could further oxidize some dihydrodiols generated from 4-ring

19 PAHs to yield tetraols. However, the amounts of reaction products obtained from small-scale

20 enzymatic assays were limited, thus preventing adequate structural characterization of the

21 hydroxylated products. In the present work, we describe the production, purification and

22 structural investigations on such products, using a *E. coli* strain overproducing the CHY-1

23 dioxygenase as a biocatalyst. We identified new oxidation products generated from pyrene

24 and fluoranthene, and further analyzed the structure of tetraols produced from chrysene and

25 benz[a]anthracene by NMR spectroscopy. Results are discussed by referring to the known 3D

1   structure of the *Sphingomonas* CHY-1 dioxygense catalytic component (Jakoncic et al.

2   2007a; Jakoncic et al. 2007b).The regioselectivity of this enzyme is also compared to that of

3   other RHDs able to attack HMW-PAHs, which have been described thus far, essentially in

4   Sphingomonads and *Mycobacteria*.

MATERIAL AND METHODS

Incubation of PAHs with recombinant cells overproducing strain CHY-1 RHD

Escherichia coli BL21(DE3) carrying plasmids pSD9 and pEB431, has been previously described (Demaneche et al. 2004)–. This strain, subsequently referred to as Bphn12, overproduces the three components of the ring-hydroxylating dioxygenase from *Sphingomona*s CHY-1. Cultures of Bphn12 (0.8 L) were grown at 37°C on LB medium to an optical density of 1.5 at 600 nm, then subjected to overnight induction with 0.2 mM IPTG at 25°C. Cells were harvested by centrifugation, washed and resuspended in the same volume of M9 medium containing 10 mM glucose. Each studied PAH was then separately provided as a 0.1g/L solution in silicone oil (Rhodorsil 47V20, Sodipro, France), added at one fifth the volume of bacterial suspension. Biphasic cultures were incubated in 2-L flasks at 25°C on a rotary shaker (200 rpm) for 23 h (45 h for pyrene).

Extraction and purification of the PAH oxidation products

Following incubation of bacteria with PAH, the biphasic suspension was immediately decanted to remove the oil phase, then centrifuged 15 min at 5,000 *g*. The dihydrodiols and other relevant PAH oxidation products were recovered from the aqueous supernatant by solid-phase extraction on C18 Bond Elut-cartridges (1g ; Varian). The cartridge was washed with 100 ml of water, then eluted with 5 ml of acetonitrile. The crude extracts thus obtained were resolved by reverse-phase HPLC and thin layer chromatography (TLC). TLC was performed on 20 x 20 cm silica-coated glass plates (Merck) developed with chloroform/acetone 80/20 by volume unless otherwise noted. After separation, compounds of interest were visualized under UV light and recovered from the silica by elution with 0.5 ml acetonitrile. HPLC was performed on a Kontron instrument equipped with a F430 absorbance detector set at two

1 appropriate wavelengths. Separation was performed on a 10 by 300 mm µBondapak C18

2 column (Millipore Waters) run in the isocratic mode at 1.5 ml/min with a water/acetonitrile

3 mixture containing either 40 or 50 % organic solvent. Benz[a]anthracene dihydrodiols, which

4 co-eluted by reverse-phase HPLC, could be separated on a 4.6 by 150 mm Zorbax RX-SIL

5 column (Agilent Technologies), isocratically eluted at 0.9 ml/min with a solvent made of

6 hexane/dioxane/ethanol in the 93/5/2 ratio. Purified products were stored dry or in 50%

7 acetonitrile in sealed vials at -20°C.

8

9 **UV absorbance recording and estimation of dihydrodiol concentrations**

10 The UV absorbance spectra of purified PAH oxidation products were recorded on appropriate

11 dilutions in pure or 50% acetonitrile using a HP8452 diode-array spectrophotometer (Agilent

12 technologies). The dihydrodiol concentrations were calculated using the following absorption

13 coefficients: ε_{278} = 57,650 $M^{-1}.cm^{-1}$ for *cis*-3,4-dihydroxy 3,4-dihydrochrysene (Boyd et al.

14 1997); ε_{280} = 66,500 $M^{-1}.cm^{-1}$ for *cis*-9,10-dihydroxy-9,10-dihydrobenzo[a]pyrene (Gibson et

15 al. 1975); ε_{263} = 31,000 $M^{-1}.cm^{-1}$ for *cis*-1,2-dihydroxy-1,2-dihydrobenz[a]anthracene and ε_{275}

16 = 37,000 $M^{-1}.cm^{-1}$ for *cis*-10,11-dihydroxy-10,11-dihydrobenz[a]anthracene (Jerina et al.

17 1984). Pyrene 4,5-dihydrodiol was estimated by using an absorption coefficient of 98,000 $M^{-1}.cm^{-1}$

18 at 260 nm, and fluoranthene 2,3-dihydrodiol was quantified using ε_{263} = 40,000 $M^{-1}.cm^{-1}$.

19

20 For the 7,8-fluoranthene dihydrodiol, the absorbance coefficients were determined as follows:

21 Taking advantage of the fact that the short-term fluoranthene oxidation reaction catalyzed by

22 purified PhnI produced >98% of 7,8-dihydrodiol ((Jouanneau et al. 2006) and see Results),

23 we carried out the complete conversion of a known amount of fluoranthene (20 µM) by

24 purified PhnI within 30 min under conditions previously described (Jouanneau et al. 2006).

25 The reaction product was extracted with ethyl acetate and dried with anhydrous sodium

1 sulfate. After solvent evaporation, the dihydrodiol was taken up in 0.5 ml acetonitrile and its

2 absorbance spectrum was recorded. The purity of the product and absence of residual

3 fluoranthene was checked by HPLC as described previously (Jouanneau et al. 2006).

4 Assuming a 40 µM concentration in the extract, the absorbance coefficient of *cis*-7,8-

5 dihydrodiol was calculated to be: ε_{334} = 10,100 M^{-1} cm^{-1} at 334 nmn; ε_{236} = 29,950 M^{-1} cm^{-1}

6 ar 236 nm and ε_{442} = 1,370 M^{-1} cm^{-1} at 442 nm.

7

8 GC/MS analyses

9 Purified PAH oxidation products were subjected to GC/MS analysis as previously described

10 (Jouanneau et al. 2006) with minor modifications. Briefly, samples were derivatized with

11 bis(trimethysilyl)trifluoroacetamide : trimethylchlorosilane (99:1) from   Macherey-Nagel,

12 prior to analysis using a HP6890 gas chromatograph coupled to a HP5973 mass spectrometer

13 (Agilent Technologies). Samples (2.5 µl) were injected into a capillary column (30-m long,

14 0.25-mm internal diameter, Varian VF-5ms) using the split mode (a split ratio of 20:1 was

15 applied). Each run was carried out at an helium flow rate of 1 ml/min, with a temperature

16 gradient from 75 to 300°C. Mass spectra were acquired in the total ion current mode. Some

17 samples were derivatized with N-butyl boronate (Sigma-Aldrich) prior to GC/MS analysis

18 performed as above.

19

20 NMR analyses of purified dihydrodiols and tetraols

21 ^{1}H, ^{13}C and [2]D-NMR spectra were recorded at 300K with a Bruker DPX 300 spectrometer

22 equipped with a QNP 5-mm probehead with a *z*-gradient coil for 2D experiments (90°: 11.0

23 µs at 0dB ^{1}H; 5.20 µs at – 6 dB ^{13}C). Samples were dissolved in methanol-*d 4* (^{1}H/[13]C 3.30/49

24 ppm) for the chrysene tetraol and fluoranthene diol, or in acetone-*d6* (^{1}H/[13]C 2.04/29.8 ppm)

25 for the benz[a]anthracene tetraol. Signal assignments were determined based on recordings of

1   gradient-assisted correlated spectroscopy (COSY) and gradient-assisted nuclear Overhauser

2   spectroscopy (NOESY) with a mixing time of 800ms, which were referred to as *cosygp* and

3   *noesygp*, respectively, in the Bruker library. A DEPT 135 sequence was performed to

4   complete carbon assignments. To assign carbons bearing a proton, a gradient-assisted

5   heteronuclear multiple quantum correlation (GRASP-HMQC) optimized for the detection of

6   the $^1J_{CH}$ (145 Hz) with ^{13}C-GARP decoupling (GARP: 85 µs, aq: 175 ms) was used.

7   Benz[a]anthracene tetraol analysis was performed by recording gradient-assisted

8   heteronuclear multiple quantum correlation (gHMQC), double quantum filtered correlated

9   spectroscopy (DQF-COSY) and gradient-assisted nuclear Overhauser spectroscopy with

10   mixing time of 150 and 300 ms on a Varian INOVA 600 spectrometer using a standard 5 mm

11   triple resonance probehead.

12

1 **RESULTS**

2

3 **Biotransformation of PAHs by *E. coli* overproducing *Sphingomonas* CHY-1 RHD**

4 Strain Bphn12 is a BL21(DE3) derivative overproducing the three components of stain CHY-

5 1 RHD namely, PhnI (oxygenase), PhnA4 (reductase) and PhnA3 (ferredoxin) (Demaneche et

6 al. 2004). It was used as a biocatalyst to oxidize fluoranthene, benz[a]anthracene (BaA),

7 chrysene and pyrene, as representative 4-ring PAHs, as well as beno[a]pyrene (BaP). In order

8 to generate sufficient PAH oxidation products for subsequent analysis, 0.96 L biphasic

9 cultures were separately incubated with each PAH for 23 h or 45 h for pyrene. Prolonged

10 incubation was avoided to limit unwanted degradation of oxidation products. These products

11 were recovered from the aqueous phase by solid-phase extraction and further purified as

12 described below.

13

14 **Identification of the fluoranthene oxidation products**

15 The oxidation products formed upon incubation of fluoranthene with Bphn12 were separated

16 by reverse-phase HPLC. Four UV-absorbing fractions displaying retention times ranging

17 between 13 min (Fraction F1) and 28 min (F4) were collected. Fraction F1 essentially

18 consisted of a single compound, yellow in color, which was further purified by thin layer

19 chromatography. This product, designated as FP1, was by far the major product formed as

20 judged from HPLC and TLC analysis of the crude extract. It showed an absorbance spectrum

21 with three maxima in the UV range and a broad maximum around 442 nm (see Fig S1A in

22 supplemental material). Fraction F2 was a mixture including some FP1 product (overlap), a

23 monohydroxyfluoranthene with a GC retention time of 20,41 min (Table 1), and a compound

24 with a distinctive R_f of 0.45 by TLC, which exhibited a mass spectrum typical of a

25 dihydrodiol (Table 1). This product was recovered in small amounts, thus precluding

1   determination of the hydroxyl positions by NMR. Its UV absorbance spectrum, with maxima

2   at 232, 260 and 268 nm and a shoulder at 250 nm, was clearly distinct from that of the *cis* 2,3-

3   dihydrodiol, although the two dihydrodiols showed almost identical GC retention times

4   (Table 1 and see below). Based on these properties, and taking into account published data on

5   fluoranthene metabolism (Kweon et al. 2007; Lopez et al. 2006; Story et al. 2001), we

6   tentatively propose that this dihydrodiol carries hydroxyls on the C1 and C2 positions.

7   Fraction F3 mainly contained a compound with a TLC R_f of 0.35, which displayed UV

8   absorbance maxima at 230, 250, 260 and 290 nm, and mass spectral features that identified it

9   as another dihydrodiol (Table 1). Its properties perfectly matched those of the previously

10   characterized *cis*-2,3-dihydroxy-2,3-dihydrofluoranthene (Rehmann et al. 2001). The last

11   HPLC fraction (F4) contained a single product, which showed the highest R_f upon TLC

12   (0.82). This compound exhibited UV absorbance (Fig. S1B) and GC/MS properties that

13   closely matched those of 8-hydroxyfluoranthene (Table 1; (Jouanneau et al. 2006)).

14   The FP1 product turned out to be unstable and was converted to 8-hydroxyfluoranthene upon

15   heating, as evidenced by UV absorbance recordings and TLC analysis. As a consequence of

16   its instability, analysis of FP1 by GC/MS almost exclusively yielded the 8-

17   hydroxyfluoranthene spectrum. Nevertheless, GC/MS analysis of a concentrated FP1 sample

18   allowed the detection of a third diol with a R_t of 20.30 min (Table 1).

19   ^{1}H-NMR analysis of the FP1 product revealed the presence of three mutually coupling groups

20   identifying eight aromatic protons, two carbinol protons and two protons of hydroxyl groups.

21   The ^{13}C-NMR and ^{1}H,[13]C-HMQC spectra further indicated that ten carbons carried a proton,

22   two of which had a specific sp^3 carbon chemical shift. The set of NMR assignments for this

23   compound is summarized in Table 2. The chemical shifts at 4.55 and 4.95 ppm were assigned

24   to the H_8 and H_7 carbinol protons, respectively. Specifically, the value of the coupling

25   constant between these vicinal protons (6.5 Hz) indicated that they were bound in a *cis*

conformation (Jerina et al, 1984 ; Rehmann et al, 2001). We therefore conclude that the main product generated by the CHY-1 dioxygenase from fluoranthene was the *cis*-7,8-dihydroxy-7,8-dihydrofluoranthene.

In a previous study, the instability of this diol led us to erroneously conclude that the purified CHY-1 dioxygenase converted fluoranthene to 8-hydroxyfluoranthene, based on GC/MS data (Jouanneau et al. 2006). In fact, the absorbance of the product formed by the RHD complex *in vitro* was quasi identical to that of the purified 7,8-dihydrodiol (Fig. S1A) and this was so, because the other oxidation products identified above were produced in very low amounts at least at the scale of our *in vitro* enzymatic reaction. Consistent with this observation, we estimated that the recovery of purified *cis* 7,8-dihydrodiol from the Bphn12 culture (8.5 μmoles based on A_{334} and $\varepsilon_{334} = 10,100$ M^{-1} cm^{-1}; see Methods) was 270-fold higher than that of the *cis* 2,3-dihydrodiol (31.2 nmoles), the dihydrodiol that ranked second by abundance in the culture extract. The conversion yields of fluoranthene into dihydrodiols are reported in Table 1.

Hence, the biotransformation of fluoranthene by strain CHY-1 RHD essentially yielded one predominant dihydrodiol hydroxylated on C7 and C8, and two minor dihydrodiols hydroxylated on the C2-C3 and, presumably, the C1-C2 positions (Fig. 1A). The two monohydroxy-fluoranthene also detected, one of which derived from the 7,8-dihydrodiol, probably arose from spontaneous dehydration reactions.

Characterization of oxidation products generated from **benz[a]anthracene and chrysene**

The oxidation products found in Bph12 cultures upon incubation with BaA were extracted and subjected to HPLC separation. Two main UV-absorbing fractions were obtained noted BA1 and BA2, which were further analyzed by TLC. The BA1 fraction was developed with a solvent consisting of 10% methanol in chloroform, resulting in the separation of a major

compound with a R_f of 0.165. The UV absorbance spectrum of this compound is shown in

supplementary figure S2D. GC/MS analysis of the tms derivate of this compound gave a

molecular mass of 584 and a spectrum consistent with a *bis-cis*-dihydrodiol or tetraol (Table

1). Two additional components with higher R_t (24.43 and 25.01 min) and lower relative

abundance showed a molecular mass of 494 [584 – OHSi(CH$_3$)$_3$] and a mass spectrum that

identified them as hydroxylated dihydrodiol derivatives of BaA (data not shown). These

compounds were probably dehydration products of the tetraol, which probably formed during

derivatization step prior to GC/MS analysis.

The ^{1}H-NMR spectrum of the BA1 product featured three mutually coupling groups

indicating the presence of eight aromatic protons, four carbinol protons and four protons of

hydroxyl groups. 2D ^{1}H,^{1}H-COSY, and ^{1}H,^{1}H-NOESY experiments allowed to define the

succession of these protons and therefore to assign all the chemical shifts. The ^{13}C-NMR and

the ^{1}H,^{13}C-HMQC spectra showed that twelve carbons carried a proton, four of which had a

specific sp^3 carbon chemical shift. The set of NMR assignments for this compound is

summarized in Table 3. The chemical shifts at 4.36, 4.63, 4.77 and 5.28 ppm were assigned to

the H_{10}, H_2 non-benzylic, and the H_{11}, H_1 benzylic protons, respectively. The values of the two

coupling constants between the carbinol protons, both at 5.4 Hz, indicated that the vicinal

protons had a *cis* conformation (Jerina et al, 1984).

In addition, no W coupling was observed between the allylic carbinol proton H_2 and the

vinylic proton H_4, suggesting that the allylic hydroxyl group had a pseudo-axial conformation.

Likewise, no coupling was detected between the allylic carbinol proton H_{10} and the vinylic

proton H_8 so that the allylic hydroxyl group would also be in a pseudo-axial conformation.

This analysis is confirmed by the coupling value of 4.5 Hz between the allylic carbinol proton

H_{10} and the vinylic proton H_9. Indeed, it has been shown that the magnitude of the coupling

corresponded to the case where the allylic hydroxyl group had a pseudo-axial conformation

1   (Jerina et al. 1976).

2   Altogether, our NMR and GC/MS data showed that the BA1 compound was a BaA tetraol

3   with two pairs of hydroxyl groups both in *cis* conformation, occupying the carbon positions

4   C1-C2 and C10-C11. Moreover, NMR data provided evidence that the hydroxyl groups on C2

5   and C10 would preferentially adopt a pseudo-axial conformation as depicted in Fig. 2.

6   The second HPLC fraction (BA2) was found to contain three dihydrodiols by GC/MS (Table

7   1). The most abundant one (60-72 %) could be isolated as a pure component upon further

8   reverse-phase HPLC, taking advantage of its slightly shorter retention time compared to that

9   of the other diols. It was identified as *cis*-1,2-BaA dihydrodiol based on its UV absorbance

10 spectrum (Fig. S2A) and mass spectral data that matched those previously reported for this

11 compound (Jerina et al., 1984). The other two diols were successfully separated by normal

12 phase HPLC separation (*Rt* of 24.5 and 28 min, respectively). They showed distinctive

13 absorbance features in the UV range (Fig. S2B and S2C) and were identified based on the

14 same criteria as above as the *cis*-8,9- and *cis*-10,11-dihydrodiols of BaA. The four BaA

15 hydroxylated products generated by the CHY-1 RHD are represented in Fig. 1B.

16 Chrysene biotransformation by Bphn12 gave essentially two products that could be easily

17 separated by HPLC. The product with the shortest retention time yielded a single band by

18 TLC (*Rf :* 0.145 with chloroform/methanol, 9/1 as solvent), and gave a UV absorbance

19 spectrum with maxima at 264, 274, 338, 350, 368 nm (Fig. S3B). As deduced from the mass

20 spectrum of the tms derivative and its molecular mass (M^+= 584), this product was identified

21 as a *bis-cis*-dihydrodiol (Table 1). As observed for the BaA tetraol, two additional GC/MS

22 peaks with a molecular mass of 494 were also detected (data not shown). Likewise, these

23 compounds probably formed by dehydration of the unstable tetraol.

24 Further characterization of this tetraol by NMR showed that it resulted from two *cis*-

25 dihydroxylation of chrysene (Table 4). In all NMR spectra (1D and 2D ^{1}H- or ^{13}C-NMR), the

1 number of signals was half that of the protons or carbon atoms (except for quaternary

2 carbons), indicating that the molecule had a symmetrical structure (Table 4). The chemical

3 shifts at 4.53 and 5.16 ppm were assigned to the H_3 (or H_9) and H_4 (or H_{10}) carbinol protons,

4 respectively. A single coupling constant at 4.8 Hz was observed between the two pairs of

5 vicinal carbinol protons, indicating that both had a *cis* conformation.

6 Unlike what was observed for the BaA tetraol, the W coupling constant between the allylic

7 carbinol proton H_3 (or H_9) and the vinylic proton H_1 (or H_7) had a value of 3.9 Hz, consistent

8 with a pseudo-equatorial conformation of the hydroxyl group. Accordingly, a coupling

9 constant < 2 Hz was found between the allylic carbinol proton H_3 and the vinylic proton H_2,

10 thus supporting the suggested conformation for the hydroxyls on C3 and C9.

11 In conclusion, our data provide evidence that one of the major product formed upon chrysene

12 oxygenation by strain CHY-1 RHD was the *cis,cis*-3,4,9,10-tetrahydroxy-3,4,9,10-

13 tetrahydrochrysene. Furthermore, NMR data indicate that the hydroxyl groups bound to C3

14 and C9 would be in a pseudo equatorial configuration.

15

16 The second HPLC fraction was found to consist of a single compound showing a UV

17 absorbance spectrum (Fig. S3A) and mass spectral data (M^+ = 406, tms derivative), which

18 closely matched those of the previously described *cis*-3,4-dihydroxy 3,4-dihydrochrysene

19 (Boyd et al. 1997). From the UV absorbance of the purified fraction (ε_{278} = 58,650 M^{-1}. cm^{-1}),

20 approx. 168 nmoles of *cis*-3,4-dihydrodiol was recovered per liter of culture. To explain the

21 occurrence of the teraol, it seems likely that the dioxygenase first attacked the substrate on the

22 C3-C4 positions, then used the dihydrodiol as substrate to form the tetraol (Fig. 1C).

23

24 Biotransformation of pyrene and benzo[a]pyrene

25 Following incubation of a Bphn12 culture with pyrene, a UV detectable product (260 nm)

1   appeared in the extract of the aqueous phase. This product was purified by HPLC and

2   analyzed by its UV absorbance spectroscopy. Its spectrum exhibited maxima at 220, 262 and

3   298 nm and closely resembled that of the *cis* 4,5-pyrene dihydrodiol, which we had

4   previously identified as generated by another RHD from a pyrene-degrading *Mycobacterium*

5   strain (Krivobok et al. 2003). GC/MS analysis confirmed the identification of the product as

6   its R_t and mass spectrum matched those of the *cis* 4,5-pyrene dihydrodiol. Compared to the

7   other substrates studied herein, pyrene yielded a relatively small amount of diol (only about

8   15 nmoles/L culture based on GC/MS estimation) within an incubation time twice as long,

9   suggesting that it was a poor substrate for strain CHY-1 RHD.

10   Benzo[a]pyrene (BaP) was converted by Bphn12 cultures into one major product that gave a

11   single peak upon HPLC analysis. The UV absorbance spectrum of this compound (Fig. S4)

12   was quite similar to that of *cis*-9,10-dihydroxy-9,10-dihydroBaP (Gibson et al., 1975).

13   GC/MS analysis of the tms derivate was consistent with the dihydrodiol structure of the

14   product (Table 1). Further analysis of the product after N-butylboronate derivatization yielded

15   a major compound with the expected molecular mass of 352 (R_t: 26.98 min) and a minor

16   component with the same molecular mass and a higher R_t (27.85 min), which accounted for

17   about 7% of the total amount of diols based on GC/MS peak area. Although the latter

18   compound was too scarce to allow rigorous identification, it might be the *cis*-7,8-dihydrodiol

19   previously found to be a secondary product formed from BaP by a similar RHD (Gibson et al.,

20   1975). Based on the A_{280} absorption of the 9,10-BaP dihydrodiol, we estimated that the

21   Bphn12 culture produced approximately 72 nmoles/L of this diol.

22

23   **DISCUSSION**

24

25   In the present study, we further explored the catalytic function of *Sphingomonas* CHY-1

1   naphthalene dioxygenase and showed that it could dihydroxylate two additional 4-ring PAHs,

2   pyrene and fluoranthene. Taking into account previous reports on this enzyme (Demaneche et

3   al. 2004; Jouanneau et al. 2006), its substrate range was thus extended to include nine PAHs

4   of the priority list made of up to 5 rings. Such a broad specificity is exceptional and most

5   likely due to the size and topology of its substrate-binding pocket, which is larger than that of

6   most known RHDs (Jakoncic et al. 2007a; Jakoncic et al. 2007b). The CHY-1 dioxygenase

7   shows close similarities with the biphenyl dioxygenase from *Sphingobium yanoikuiyae* B1,

8   the two enzymes sharing a high level of sequence identity (91.0% and 96.6% for the alpha

9   and beta subunits, respectively), an almost identical 3D structure (Ferraro et al. 2007;

10   Jakoncic et al. 2007b) and a comparable propensity to attack HMW-PAHs ((Jouanneau et al.

11   2006; Yu et al. 2007) and references cited below). Yet, there are differences of substrate

12   preference, biphenyl being the best substrate of the latter enzyme, whereas naphthalene was

13   preferentially utilized by strain CHY-1 RHD. This suggested that subtle structural differences

14   accounted for the observed changes in substrate preference.

15   With the purified CHY-1 dioxygenase, it was observed that the rate of substrate oxidation was

16   inversely correlated with the substrate size (Jouanneau et al. 2006). In the present study, we

17   found that substrates of similar size underwent quite different oxidation rates. From the

18   conversion yields of the studied PAHs (Table 1), the substrate preference of the CHY-1

19   dioxygenase would respect the following order: fluoranthene > benz[a]anthracene > chrysene

20   > benzo[a]pyrene > pyrene. This observation indicated that steric constraints other than those

21   merely due to substrate size affected the rate of the dioxygenation reaction. In PAH-degrading

22   *Mycobacteria*, multiple RHDs with relatively narrow specificities were found.

23   *Mycobacterium* sp. strain 6PY1 synthesized two RHDs showing marked preferences for

24   phenanthrene and pyrene, respectively (Krivobok et al. 2003). In *M. vanbalenii* PYR-1, two

25   RHDs that exhibited narrow specificities for pyrene and fluoranthene, respectively, were

subjected to molecular modeling as a means to try to correlate substrate specificity with the shape of the substrate-binding pocket (Kweon et al. 2010). However, 3D structure determination is needed to draw relevant conclusions on structure-function correlations regarding these enzymes.

Our results indicate that fluoranthene is a good substrate for the CHY-1 dioxygenase relative to other 4-ring PAHs in accordance with previous data obtained with the purified enzyme (Jouanneau et al. 2006). The enzyme proved capable of attacking the four-ring hydrocarbon on three positions, indicating that fluoranthene can enter the substrate-binding pocket in three different ways. Likewise, BaA gave rise to three dihydrodiols, which were found to correspond to three possible orientations of the substrate at the active site as predicted from docking experiments with the 3D structure of the oxygenase component (Jakoncic et al., 2007a). With fluoranthene as substrate, however, the orientation yielding the *cis*-7,8-dihydrodiol was highly preferred since other diols were found in proportions <1%. Despite the fact that strain CHY-1 cannot grow on fluoranthene (Willison , 2004), our findings suggest that it might be degraded further by cleavage of the aromatic ring adjacent to the C7-C8 bond. In contrast, *Mycobacterium* species preferentially metabolize fluoranthene by another route involving an initial attack on the C2-C3 carbon positions (Rehmann et al., 2001; Lopez et al., 2006; Kweon e al., 2007). This difference is certainly related to the catalytic properties of the RHD oxidizing fluoranthene in PAH-degrading *Mycobacteria*, which, in *M. vanbalenii* PYR-1, has been shown to produce almost exclusively the *cis* 2,3-dihydrodiol (Kim et al., 2006).

BaA also appeared as a fairly good substrate for strain CHY-1 dioxygenase as judged from the recovery of oxidation products. The enzymatic reaction yields three dihydrodiols and a tetraol, which has been characterized as *cis,cis*-1,2,10,11-tetrahydroxy 1,2,10,11-tetrahydroBaA based on MS and NMR data. The absolute configuration of this compound

1   could not be determined, but it seems likely that the pairs of hydroxyls bonded on C1-C2 and

2   C10-C11 be oriented on opposite faces of the molecule (Fig. 2). This assumption is deduced

3   from our previous observation that the tetraol is produced by the purified RHD either from the

4   1,2- or the 10,11-dihydrodiol, which have unique configurations (Fig. 1B; Jouanneau et al.,

5   2006). Among other RHDs able to oxidize BaA, the *S. yanoikuyae* B1 RHD mostly resembles

6   the CHY-1 enzyme in that it produces the same three dihydrodiols from BaA (Jerina et al.,

7   1984). Formation of the relevant BaA tetraol was however not reported, although strain B1

8   RHD was shown to form another tetraol from the BaA 5,6-dihydrodiol (Boyd et al., 2006).

9   Besides, the RHD from both strains were shown to convert another 4-ring diol, chrysene 3,4-

10   dihydrodiol, to a tetraol hydroxylated in positions 3,4,9 and 10 (Fig. 2C; Boyd et al., 1999).

11   Hence, there are strong apparent similarities in catalytic activity and regioselectivity between

12   the two enzymes, which likely reflect their closely related structures. As previously

13   underlined for the strain B1 RHD, the hydroxylation of 4-ring substrates preferentially occurs

14   on the bay sides of the molecules (Boyd et al. 1999), a propensity certainly linked to the form

15   and topology of the substrate-binding pocket, which determines the orientation of the

16   substrate and thereby, the enzyme regioselectivity (Jakoncic et al., 2007a). The initial attack

17   of BaA in *Mycobacterium* strains appears to involve RHDs with a different selectivity. Strain

18   RGII-135 was found to convert BaA into two dihydrodiols, the most abundant of which being

19   hydroxylated on C5-C6 (Schneider et al., 1996). In *M.. vanbalenii* PYR-1, the two RHDs able

20   to attack HMW-PAHs exhibited little activity towards BaA, and converted it to the 5,6- and

21   10,11-dihydrodiols (Kim 2006, Kweon 2010).

In this work, we observed that the CHY-1 dioxygenase showed a better activity with BaP as

substrate than with pyrene, although the latter substrate is smaller. Considering the structural

similarities between the two polyaromatic substrates, this result is intriguing and might be

explained by assuming that the additional ring in BaP helps this substrate to be processed at th

1   enzyme active site. Accordingly, docking experiments performed with the dioxygenase 3D

2   structure previously showed that BaP fitted into the substrate-binding pocket in only one

3   position, where the additional ring was proximal to the iron atom at the active site (Jakoncic

4   et al. 2007a). This position of BaP explains why it is preferentially hydroxylated on the C9-

5   C10 positions. On the other hand, it is conceivable that the access of the compact 4-ring

6   molecule of pyrene to the enzyme active site might be hindered by steric constraints due to

7   the narrow shape of the substrate-binding pocket near the iron atom. Beyond this trait

8   particular to the CHY-1 dioxygenase, examples of RHDs more active on HMW-PAHs than

9   on 2- or 3-ring hydrocarbons have been described, especially in *Mycobacterium* 6PY1

10 (Krivobok et al. 2003) and *M. vanbalenii* PYR-1 (Kweon et al. 2010)..

11 The broad specificity of the dioxygenase described in this study, especially its ability to attack

12 HMW-PAHs, makes it a valuable biocatalyst, potentially useful in bioremediation of

13 contaminated sites. The enzyme is also of interest in that it converts aromatic substrates to

14 pure *cis*-dihydrodiols (or *bis,cis*-dihydrodiols). In this respect, it shares with the *S. yanoikuyae*

15 B1 dioxygenase, the ability to convert 3- and 4-ring compounds to chiral dihydrodiols or

16 tetraols, some of which might be useful for the synthesis of fine chemicals and

17 pharmaceuticals (Boyd et al. 2006; Boyd et al. 2008; Boyd et al. 1999).

18

23

24 Conflict of interest The authors declare that they have no competing interests.

References

Bamforth SM, Singleton I (2005) Bioremediation of polycyclic aromatic hydrocarbons: current knowledge and future directions. J Chem Technol Biotechnol 80:723-736

Boyd DR, Sharma ND, Agarwal R, Resnick SM, Schocken MJ, Gibson DT, Sayer JM, Yagi H, Jerina DM (1997) Bacterial dioxygenase-catalysed dihydroxylation and chemical resolution routes to enantiopure *cis*-dihydrodiols of chrysene. J Chem Soc-Perkin Trans 1(11):1715-1723

Boyd DR, Sharma ND, Belhocine T, Malone JF, McGregor S, Allen CCR (2006) Dioxygenase-catalysed dihydroxylation of arene cis-dihydrodiols and acetonide derivatives: a new approach to the synthesis of enantiopure tetraoxygenated bioproducts from arenes. Chem Commun(47):4934-4936

Boyd DR, Sharma ND, Coen GP, Hempenstall F, Ljubez V, Malone JF, Allen CCR, Hamilton JTG (2008) Regioselectivity and stereoselectivity of dioxygenase catalysed cis-dihydroxylation of mono- and tri-cyclic azaarene substrates. Org Biomol Chem 6(21):3957-3966

Boyd DR, Sharma ND, Hempenstall F, Kennedy MA, Malone JF, Allen CCR, Resnick SM, Gibson DT (1999) *bis-cis*-Dyhydrodiols: a new class of metabolites resulting from biphenyl dioxygenase-catalyzed sequential asymetric *cis*-dihydroxylation of polycyclic arenes and heteroarenes. J Org Chem 64: 4005-4011

Demaneche S, Meyer C, Micoud J, Louwagie M, Willison JC, Jouanneau Y (2004) Identification and functional analysis of two aromatic ring-hydroxylating dioxygenases from a *Sphingomonas* strain degrading various polycyclic aromatic hydrocarbons. Appl Environ Microbiol 70:6714-6725

Doyle E, Muckian L, Hickey AM, Clipson N (2008) Microbial PAH Degradation. Adv Appl Microbiol 65:27-66

1   Ferraro DJ, Brown EN, Yu CL, Parales RE, Gibson DT, Ramaswamy S (2007) Structural

2   investigations of the ferredoxin and terminal oxygenase components of the biphenyl

3   2,3-dioxygenase from *Sphingobium yanoikuyae* BI. BMC Struct Biol 7(10)

4   Gibson DT, Mahadevan V, Jerina DM, Yogi H, Yeh HJ (1975) Oxidation of the carcinogens

5   benzo [a] pyrene and benzo [a] anthracene to dihydrodiols by a bacterium. Science

6   189(4199):295-297

7   Heitkamp MA, Freeman JP, Miller DW, Cerniglia CE (1988) Pyrene degradation by a

8   *Mycobacterium* sp.: identification of ring oxidation and ring fission products. Appl

9   Environ Microbiol 54:2556-2565

10   Jakoncic J, Jouanneau Y, Meyer C, Stojanoff V (2007a) The catalytic pocket of the ring-

11   hydroxylating dioxygenase from *Sphingomonas* CHY-1. Biochem Biophys Res

12   Commun 352:861-866

13   Jakoncic J, Jouanneau Y, Meyer C, Stojanoff V (2007b) The crystal structure of the ring-

14   hydroxylating dioxygenase from *Sphingomonas* CHY-1. Febs J 274:2470-2481

15   Jerina DM, Selander H, Yagi H, Wells MC, Davey JF, Mahadevan V, Gibson DT (1976)

16   Dihydrodiols from anthracene and phenathrene. J Am Chem Soc 98(19):5988-5996

17   Jerina DM, Vanbladeren PJ, Yagi H, Gibson DT, Mahadevan V, Neese AS, Koreeda M,

18   Sharma ND, Boyd DR (1984) Synthesis and absolute-configuration of the bacterial

19   *cis*-1,2-dihydrodiol, *cis*-8,9-dihydrodiol, and *cis*-10,11-dihydrodiol metabolites of

20   benz[a]anthracene formed by a strain of *Beijerinckia*. J Org Chem 49:3621-3628

21   Jouanneau Y, Martin F, Krivobok S, Willison JC (2011) Ring-hydroxylating dioxygenases

22   involved in PAH biodegradation : structure, function and biodiversity. In: Koukkou AI

23   (ed) Microbial bioremediation of non metals: current research. Caister Academic

24   Press, Norflok, UK, pp 149-175

1   Jouanneau Y, Meyer C, Jakoncic J, Stojanoff V, Gaillard J (2006) Characterization of a

2   naphthalene dioxygenase endowed with an exceptionally broad substrate specificity

3   toward polycyclic aromatic hydrocarbons. Biochemistry 45(40):12380-12391

4   Juhasz AL, Naidu R (2000) Bioremediation of high molecular weight polycyclic aromatic

5   hydrocarbons: a review of the microbial degradation of benzo a pyrene. Intern

6   Biodeter Biodeg 45:57-88

7   Karlsson A, Parales JV, Parales RE, Gibson DT, Eklund H, Ramaswamy S (2003) Crystal

8   structure of naphthalene dioxygenase: side-on binding of dioxygen to iron. Science

9   299(5609):1039-1042

10   Kim SJ, Kweon O, Jones RC, Freeman JP, Edmondson RD, Cerniglia CE (2007) Complete

11   and integrated pyrene degradation pathway in *Mycobacterium vanbaalenii* PYR-1

12   based on systems biology. J Bacteriol 189:464-472

13   Krivobok S, Kuony S, Meyer C, Louwagie M, Willison JC, Jouanneau Y (2003)

14   Identification of pyrene-induced proteins in *Mycobacterium* sp. 6PY1 : Evidence for

15   two ring-hydroxylating dioxygenases. J Bacteriol 185:3828-3841

16   Kunihiro M, Ozeki Y, Nogi Y, Hamamura N, Kanaly RA (2013) Benz[a]anthracene

17   biotransformation and production of ring fission products by *Sphingobium* sp. strain

18   KK22. Appl Environ Microbiol 79:4410-4420

19   Kweon O, Kim S-J, Baek S, Chae J-C, Adjei M, Baek D-H, Kim Y-C, Cerniglia C (2008) A

20   new classification system for bacterial Rieske non-heme iron aromatic ring-

21   hydroxylating oxygenases. BMC Biochem 9:11

22   Kweon O, Kim S-J, Jones RC, Freeman JP, Adjei MD, Edmondson RD, Cerniglia CE (2007)

23   A polyomic approach to elucidate the fluoranthene-degradative pathway in

24   *Mycobacterium vanbaalenii* PYR-1. J Bacteriol 189:4635-4647

1   Kweon O, Kim SJ, Freeman JP, Song J, Baek S, Cerniglia CE (2010) Substrate specificity

2   and structural characteristics of the novel Rieske nonheme iron aromatic ring-

3   hydroxylating oxygenases NidAB and NidA3B3 from *Mycobacterium vanbaalenii*

4   PYR-1. mBio 1(2) e00135-10-e00135-20

5   Lopez Z, Vila J, Minguillon C, Grifoll M (2006) Metabolism of fluoranthene by

6   *Mycobacterium* sp strain AP1. Appl Microbiol Biotechnol 70:747-756

7   Lu X-Y, Zhang T, Fang HH-P (2011) Bacteria-mediated PAH degradation in soil and

8   sediment. Appl Microbiol Biotechnol 89:1357-1371

9   Lyu Y, Zheng W, Zheng T, Tian Y (2014) Biodegradation of polycyclic aromatic

10   hydrocarbons by *Novosphingobium pentaromativorans* US6-1. Plos One 9(7)

11   doi:10.1371/journal.pone.0101438

12   Maeda AH, Nishi S, Hatada Y, Ozeki Y, Kanaly RA (2014) Biotransformation of the high-

13   molecular weight polycyclic aromatic hydrocarbon (PAH) benzo k fluoranthene by

14   *Sphingobium* sp strain KK22 and identification of new products of non-alternant PAH

15   biodegradation by liquid chromatography electrospray ionization tandem mass

16   spectrometry. Microbial Biotechnol 7:114-129

17   Nam JW, Nojiri H, Yoshida T, Habe H, Yamane H, Omori T (2001) New classification

18   system for oxygenase components involved in ring- hydroxylating oxygenations.

19   Biosci Biotechnol Biochem 65:254-263.

20   Parales RE, Resnick SM (2006) Aromatic ring hydroxylating dioxygenases. In: Ramos JL,

21   Levesque RC (eds) Pseudomonas. vol 4. Springer, pp 287-340

22   Peng RH, Xiong AS, Xue Y, Fu XY, Gao F, Zhao W, Tian YS, Yao QH (2008) Microbial

23   biodegradation of polyaromatic hydrocarbons. FEMS Microbiol Rev 32(6):927-55

1   Rehmann K, Hertkorn N, Kettrup AA (2001) Fluoranthene metabolism in *Mycobacterium* sp

2   strain KR20: identity of pathway intermediates during degradation and growth.

3   Microbiology-Sgm 147:2783-2794

4   Schneider J, Grosser R, Jayasimhulu K, Xue W, Warshawsky D (1996) Degradation of

5   pyrene, benz[a]anthracene, and benzo[a]pyrene by *Mycobacterium* sp. strain RJGII-

6   135, isolated from a former coal gasification site. Appl Environ Microbiol 62:13-19

7   Story SP, Parker SH, Hayasaka SS, Riley MB, Kline EL (2001) Convergent and divergent

8   points in catabolic pathways involved in utilization of fluoranthene, naphthalene,

9   anthracene, and phenanthrene by *Sphingomonas paucimobilis* var. EPA505. J Ind

10   Microbiol Biotechnol 26(6):369-382

11   Vila J, Lopez Z, Sabate J, Minguillon C, Solanas AM, Grifoll M (2001) Identification of a

12   novel metabolite in the degradation of pyrene by *Mycobacterium* sp strain AP1:

13   Actions of the isolate on two- and three-ring polycyclic aromatic hydrocarbons. Appl

14   Environ Microbiol 67:5497-5505

15   Willison JC (2004) Isolation and characterization of a novel sphingomonad capable of growth

16   with chrysene as sole carbon and energy source. FEMS Microbiol Lett 241:143-150

17   Yu CL, Liu W, Ferraro DJ, Brown EN, Parales JV, Ramaswamy S, Zylstra GJ, Gibson DT,

18   Parales RE (2007) Purification, characterization, and crystallization of the components

19   of a biphenyl dioxygenase system from *Sphingobium yanoikuyae* B1. J Ind Microbiol

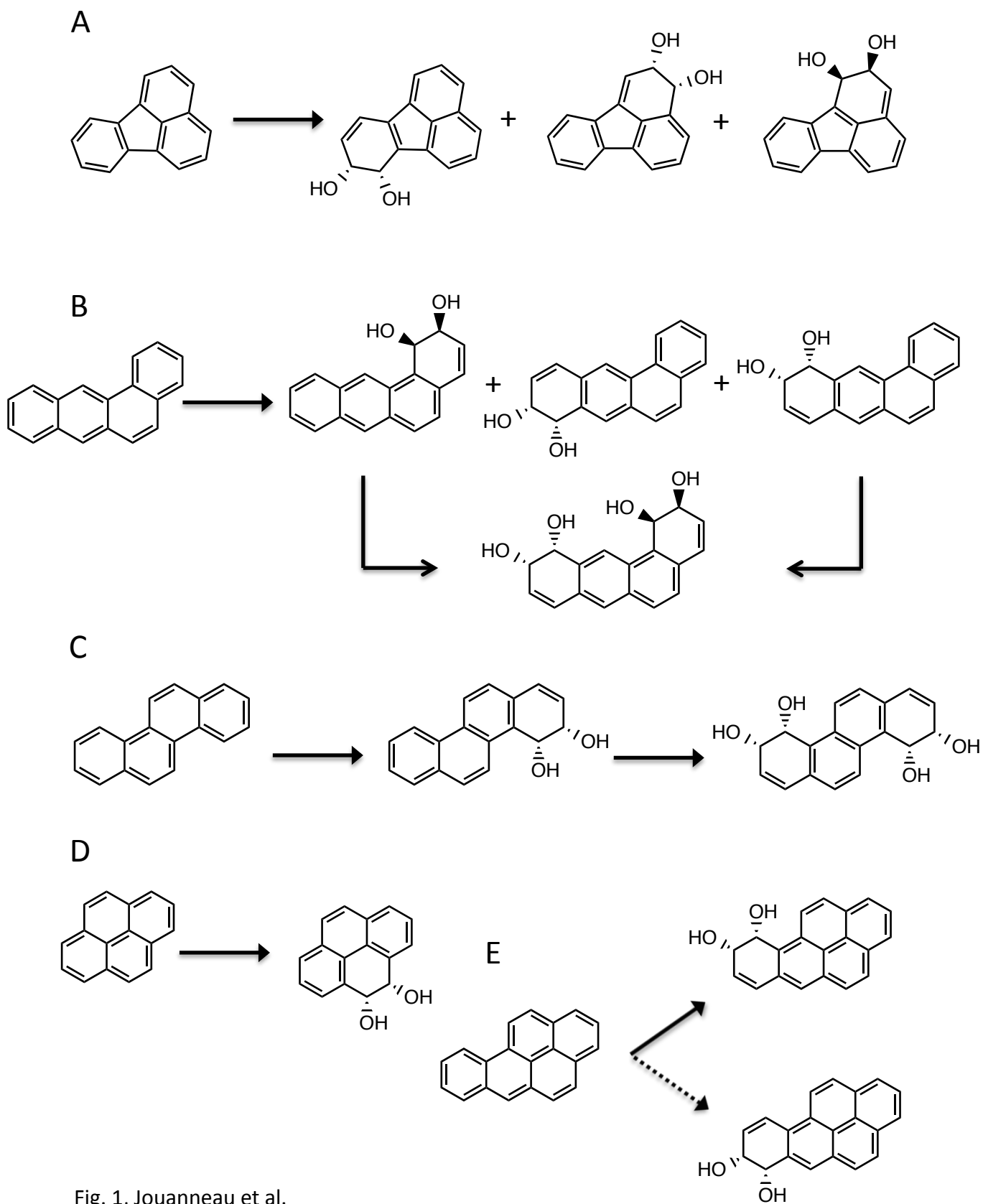20   Biotechnol 34(4):311-324

21

A

B

C

D

E

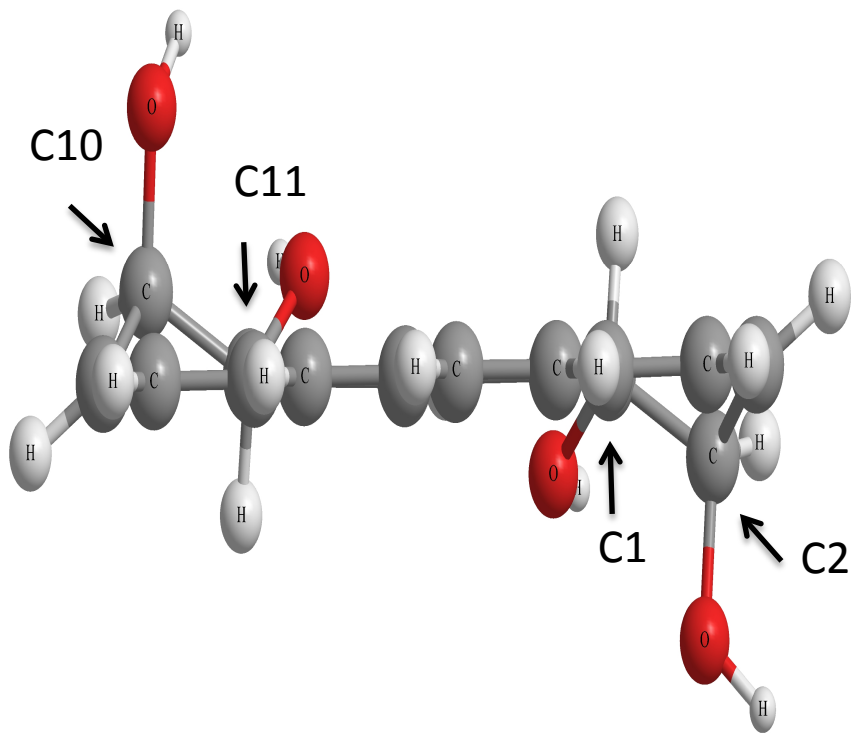Fig. 1, Jouanneau et al.

Fig. 2, Jouanneau et al.

Fig. 2, Jouanneau et al.

Supplemental figures to :

Applied Microbiology and Biotechnology

Dihydroxylation of four- and five-ring aromatic hydrocarbons by the naphthalene

dioxygenase from *Sphingomonas* CHY-1

Yves Jouanneau[1,2,3], Christine Meyer[1,2,3], and Nicolas Duraffourg[1,2,3]

[1] CEA, DSV, iRTSV, Chimie et Biologie des Métaux, F-38054 Grenoble, France.

[2] CNRS, UMR 5249, Grenoble, France.

[3] Univ. Grenoble Alpes, F-38000 Grenoble, France

Corresponding author:

    Yves Jouanneau

    LCBM/iRTSV, CEA-Grenoble

    F-38054 Grenoble Cedex 9, France.

    Tel. : 33 (0)4 38 78 43 10; Fax : 33 (0)4 38 78 54 87

    Email : yves.jouanneau@cea.fr
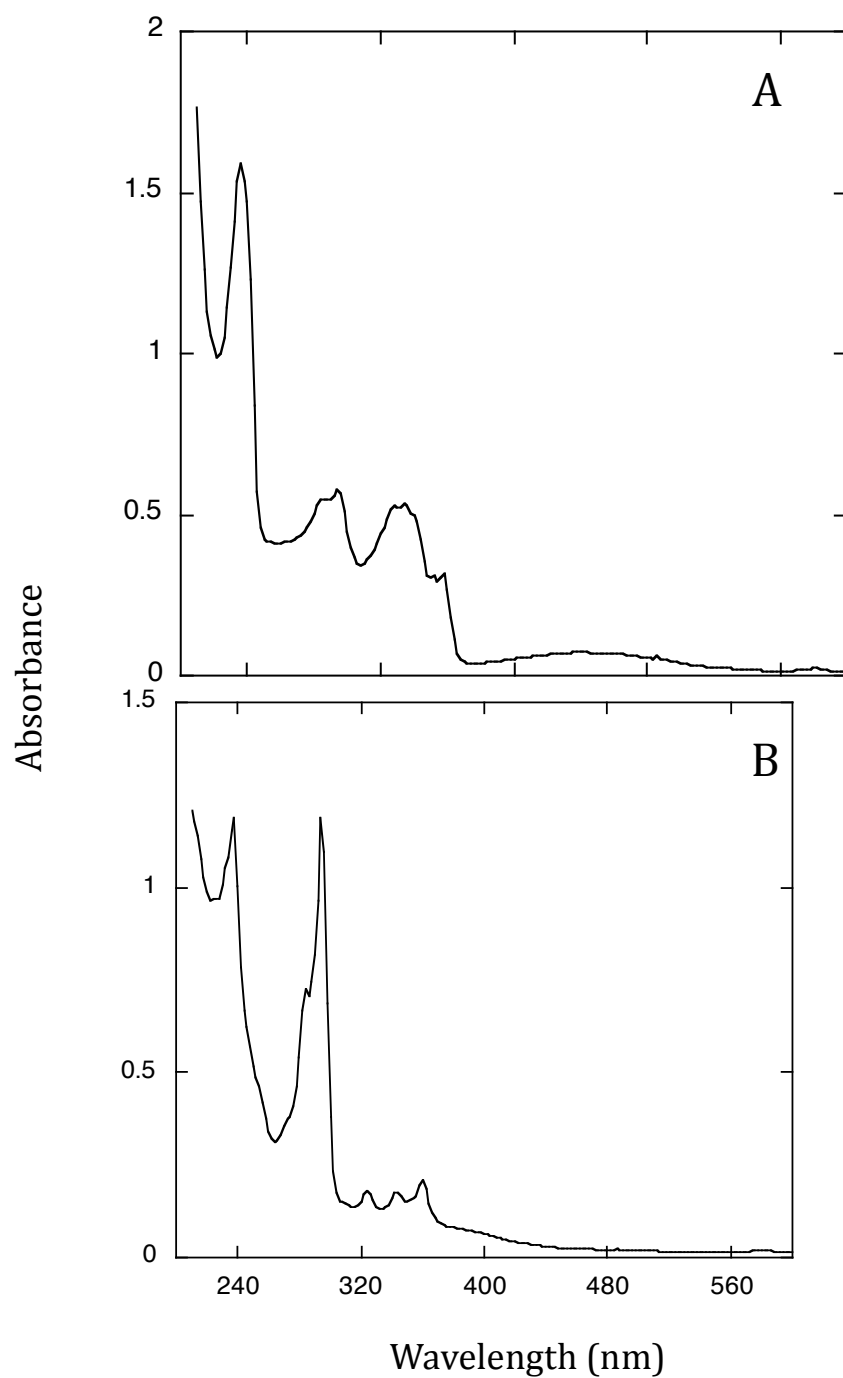
Figure S1 : Absorbance spectra of two main oxidation products of fluoranthene
A; *cis*-7,8-dihydroxy-7,8-dihydrofluoranthene, 53 µM ; B: 8-hydroxyfluoranthene. Both
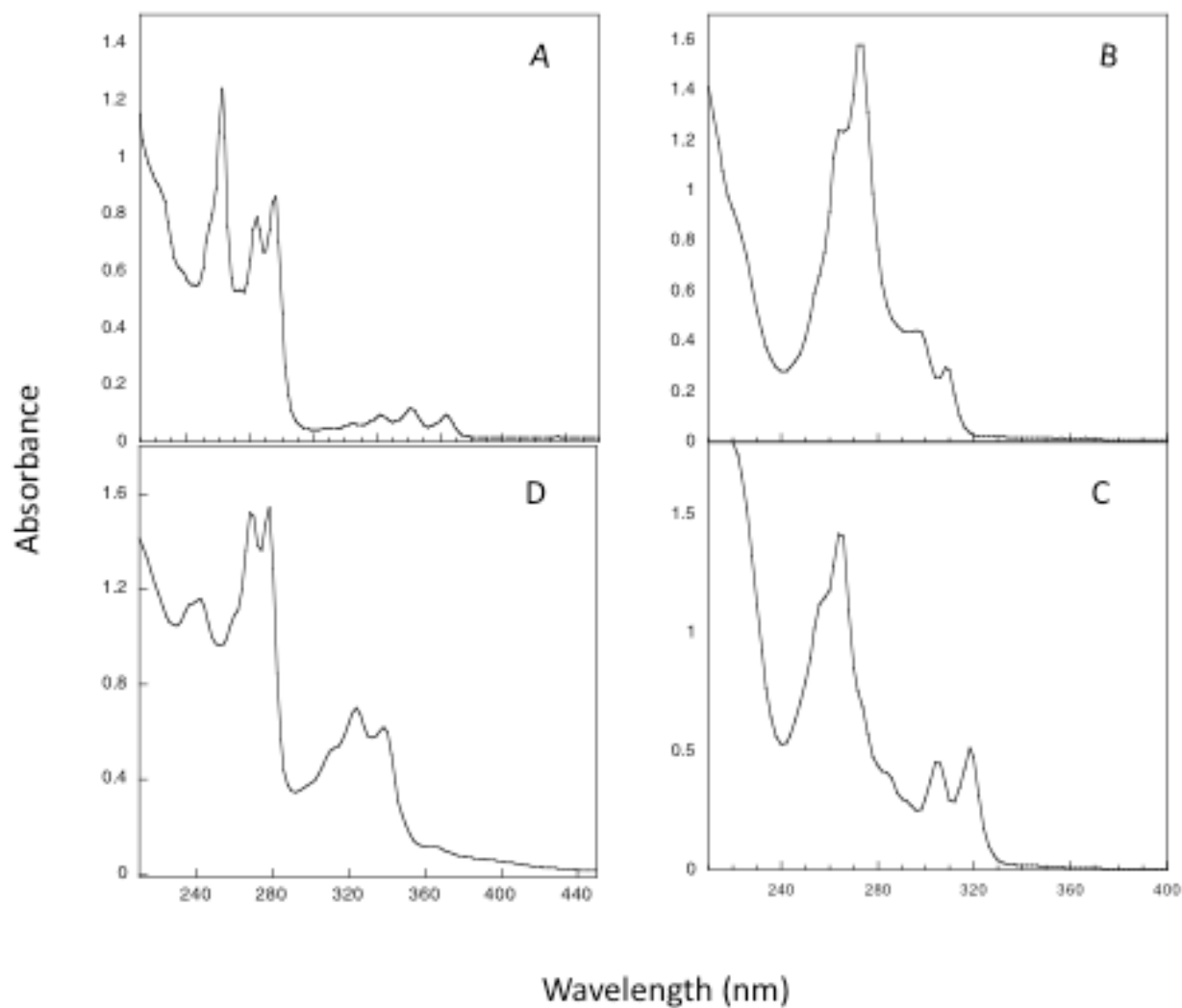spectra were recorded from solutions in acetonitrile.

Figure S2: Absorbance spectra of benz[a]anthracene oxidation products

A: *cis*-1,2-dihydrodiol; B: *cis*-10,11-dihydrodiol; C: *cis*-8,9-dihydrodiol; D: *cis,cis*-1,2,10,11-tetraol. All samples were in acetonitrile, with the dihydrodiol concentration being approx.. 40 µM.
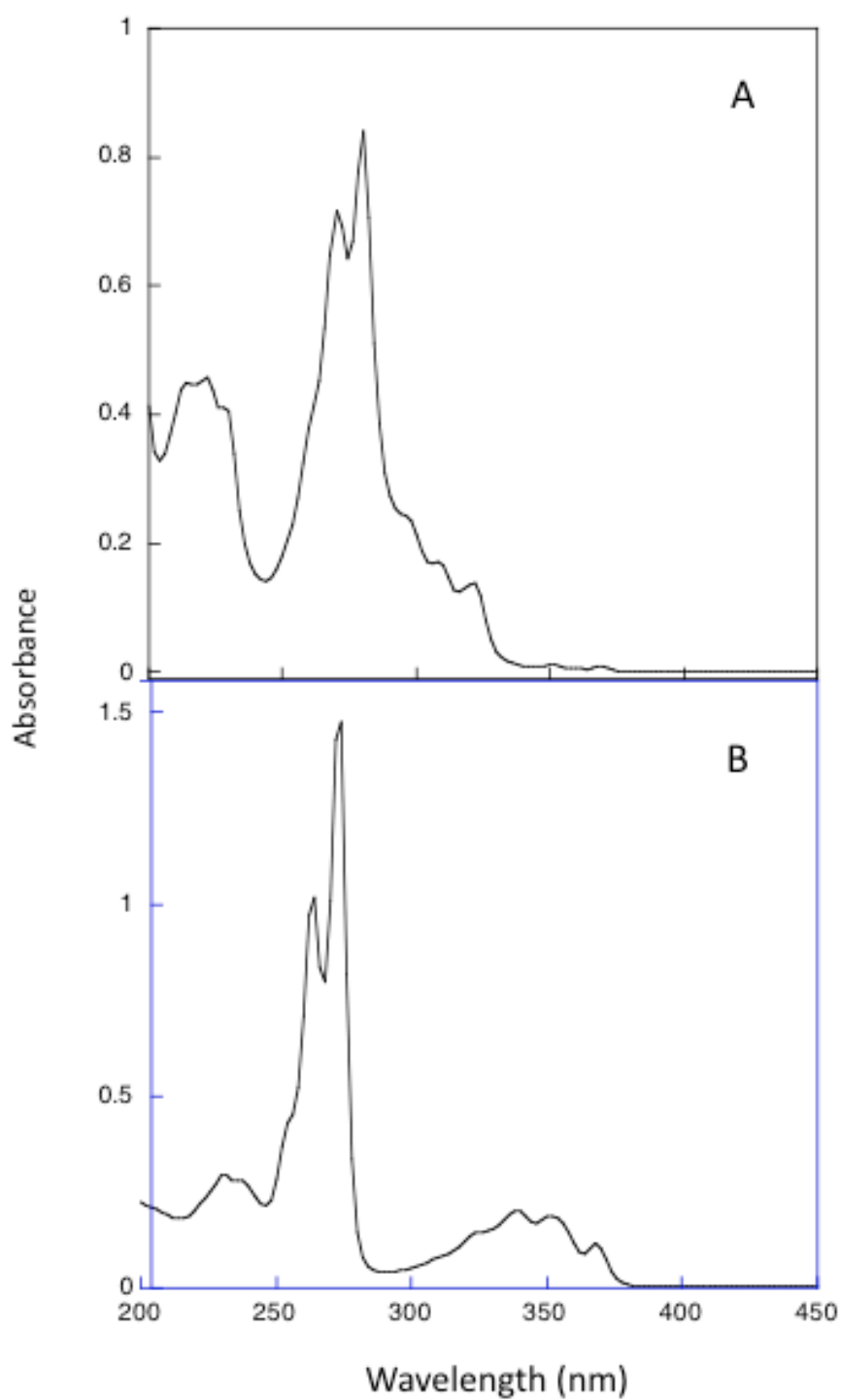
Figure S3: UV absorbance spectra of the dihydrodiol and tetraol generated from chrysene

A: *cis*-3,4-dihydroxy-3,4-dihydrochrysene; B: *cis,cis*-3,4,9,10-chrysene tetraol. Samples were in acetonitrile.
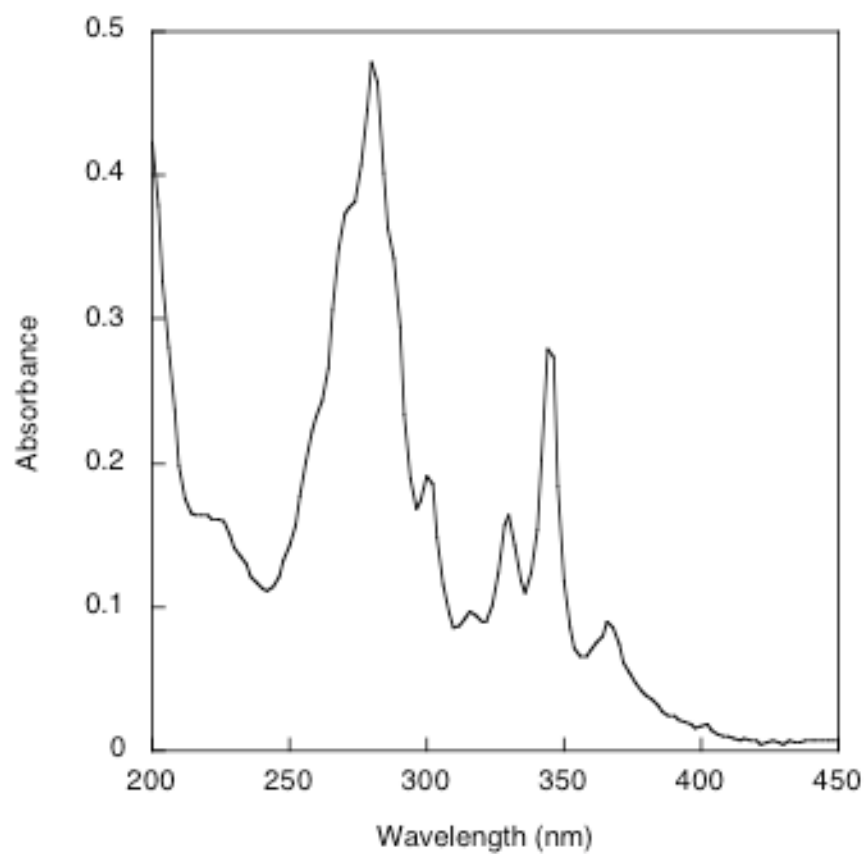
Figure S4: Absorbance spectrum of the *cis*-9,10-dihydrodiol formed from benzo[a]pyrene.

The sample concentration was 7.1 µM in acetonitrile.